Applied Physics B (2026) 132:82
https://doi.org/10.1007/s00340-026-08692-3

Applied Physics B
Lasers and Optics

RESEARCH

Green external-cavity diode lasers for Raman spectroscopy: tunability, linewidth, and performance comparison

Julia Lukaszewski[1] · Enrico Dietz[1] · Susanne Schröder[1] · Maximilian Buder[1] · Heinz-Wilhelm Hübers[1]

Received: 31 March 2026 / Accepted: 19 May 2026

Abstract

The implementation and characterization of green external cavity diode lasers (ECDL) in Littrow configuration is presented. It is specifically developed for Raman spectroscopy. Eight distinct green laser diodes are systematically characterized and compared: six broad-area diodes and two transverse single-mode diodes. All diodes achieve wide tuning ranges between 8 nm and 12 nm and output powers of more than 100 mW. One of the transverse single-mode diodes reached 45 mW maximum output power, which is sufficient for Raman measurements. Preliminary Raman measurements using a broad-area diode laser demonstrate the feasibility of this ECDL setup for spectroscopic applications.

1 Introduction

Laser diodes have become indispensable as cost-effective, energy-efficient, and highly reliable laser sources across a wide range of applications [1, 2]. Their compact design, combined with a low étendue, facilitates straightforward integration into optical systems, while their direct electrical modulation capability enables precise control of emission properties [1]. Diode lasers offer good electrical-to-optical conversion efficiencies (often exceeding 30–50%), long operational lifetimes (>10.000 hours), and minimal heat dissipation, making them ideal for space- and power-constrained environments [2]. Additionally, advances in semiconductor materials have expanded their spectral coverage from the ultraviolet to the mid-infrared [1, 2], allowing tailored excitation wavelengths for spectroscopic techniques.

✉ Julia Lukaszewski
Julia.Lukaszewski@dlr.de

Enrico Dietz
Enrico.Dietz@dlr.de

Susanne Schröder
Susanne.Schroeder@dlr.de

Maximilian Buder
Maximilian.Buder@dlr.de

Heinz-Wilhelm Hübers
Heinz-Wilhelm.Huebers@dlr.de

[1] Institute of Space Research, German Aerospace Center, DLR, Rutherfordstraße 2, 12489 Berlin, Germany

Among the promising applications of green laser diodes is Raman spectroscopy, a non-destructive technique for analyzing the molecular composition and structure of materials. Traditionally, frequency-doubled neodymium lasers (e.g., at 532 nm) have dominated this field [3]. However, green laser diodes present a compelling alternative, particularly when compared to near-infrared excitation (e.g., at 785 nm). Green excitation enables the detection of Raman shifts across a broad wavenumber range (> 4000 cm^{-1}) using silicon-based CCD or CMOS detectors [4]. The broad emission bandwidth of laser diodes, which is sensitive to temperature fluctuations and operating current, however, often limits their use in high-resolution spectroscopic techniques [5, 6]. This limitation can be overcome through the integration of an external cavity, which enables spectral narrowing and wavelength tunability [7–9]. A particularly simple approach involves the Littrow configuration, where a diffraction grating is positioned to reflect the first-order diffracted beam back into the diode, while the zeroth-order serves as the output beam [10, 11]. By rotating the grating, the emission wavelength can be precisely tuned within the gain bandwidth of the diode, typically spanning a few nanometers [7, 8]. This configuration, long established for red and infrared diodes, has been successfully adapted to blue and green wavelengths following the commercial availability of corresponding laser diodes [5, 6]. Furthermore, the tunability of external-cavity laser diodes facilitates advanced techniques such as shifted-excitation Raman difference spectroscopy (SERDS). SERDS mitigates fluorescence interference, a common challenge in Raman

Published online: 28 May 2026

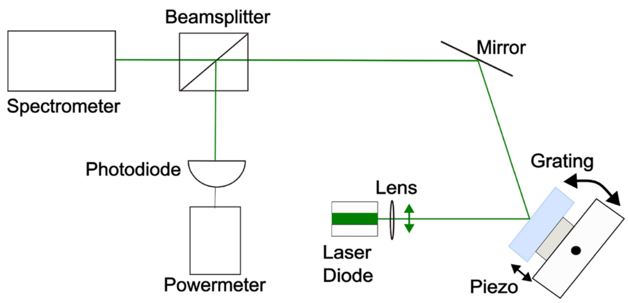

Fig. 1 Sketch of the external-cavity laser in Littrow configuration. The diffraction grating that is mounted on a piezo actuator enables fine adjustment of the cavity length. The green arrow indicates the fast axis of the laser diode, the black arrows show grating rotation (wavelength tuning) and piezo-driven external cavity length adjustment

Table 1 Diodes used in this paper. MM are broad-area diodes and SM transverse single mode diodes

Name	Supplier	Wavelength	Type
A	Lasertree	530nm	MM
B	Lasertree	525nm	MM
C	Sharp	520nm	MM
D	Sharp	520nm	SM
E	Sharp	520nm	MM
F	Osram	520nm	SM
G	Nichia	532nm	MM
H	Lasertree	530nm	MM

measurements, by exploiting the difference between spectra acquired at two closely spaced wavelengths (typically separated by 1 nm) [12]. This approach has been shown to significantly enhance the signal-to-noise ratio and therefore enabling the extraction of weak Raman signals in the presence of strong fluorescent backgrounds [12]. In recent years, Raman spectroscopy has gained attraction as an in-situ analytical tool for mineralogical analysis in space missions, enabling the direct characterization of planetary bodies without the need for sample preparation. The first two extraterrestrially employed Raman instruments are both onboard NASA's Perseverance rover and have been measuring the Martian surface since landing in 2021 [13–15]. While SHERLOC (Scanning Habitable Environments for Raman and Luminescence for Organics and Chemicals) on the robotic arm is using deep UV excitation, SuperCam Raman is using the frequency-doubled, pulsed Nd:YAG laser at 532 nm that is normally used at 1064 nm for laser-induced breakdown spectroscopy (LIBS). Two other Raman instruments that were developed for in-situ Raman spectroscopy on Mars and on the Martian moon Phobos, respectively, are the RLS (Raman Laser Spectrometer) [16] for the Rosalind Franklin Rover of the ExoMars mission currently scheduled for late 2028 and the RAman spectrometer for MMX, short RAX [17–19] for the IDEFIX rover [20] of JAXA's Martian Moons eXploration mission MMX that will launch in late 2026. Both are using a compact, continuous wave frequency-doubled Nd:YAG laser at 532 nm that was developed for RLS [21]. For Raman applications in space, laser sources must not only meet stringent optical requirements but also withstand the harsh environmental conditions of space, including extreme vibrations, thermal cycling, and radiation exposure, e.g. [22, 23]. The development of space-qualified diode laser systems, combining spectral purity, tunability, and robustness represents a critical step toward deploying Raman spectroscopy on future planetary rovers and landers. This paper presents our first successful implementation of a green (520 - 535 nm) external cavity diode laser (ECDL) in Littrow configuration, specifically designed to serve as a spectrally narrowed laser source for Raman spectroscopy with potential suitability for space applications. To be fully compatible with our RAX instrument, we aim at achieving stable output at 532 nm, though smaller wavelengths down to about 525 nm could still be used with only minor adaptions to the instrument design. We systematically evaluated eight different laser diodes based on key criteria such as emission wavelength, optical output power, spectral linewidth, and tuning range. Additionally, diffraction gratings with differing reflectivities were investigated to assess their impact on the overall system design and performance. Our results demonstrate the feasibility of the ECDL setup for Raman measurements, as evidenced by initial spectroscopic data obtained with the system. Finally, we discuss prospects for further optimization, outline conceptual advancements, and highlight ongoing developments to improve the laser's performance and applicability.

2 Experimental setup

Figure 1 shows the schematic of the experimental setup with the ECDL in Littrow configuration. The emitted light from the laser diode is collimated and directed onto the diffraction grating. While two diodes (B and H see Table 1) feature a lens integrated into their housing, the other diodes were collimated using aspheric lenses with focal lengths ranging from 4.5 to 5.5 mm. In all cases the resulting beam width is quite similar, measuring approximately 2 to 3 mm. The first-order diffracted beam is directly coupled back into the diode. The zeroth-order diffracted beam is redirected by a mirror, then divided by a beamsplitter, with one portion directed to a photodiode for optical power monitoring and the remaining light coupled into a spectrometer for spectral analysis. To enable fine tuning of the external cavity length and stabilize the laser in single-mode operation, a Piezo actuator was mounted behind the grating. It enables movement of the grating along its surface normal by approximately 2 μm, as indicated by the arrow in Fig. 1. Two holographic diffraction gratings with different reflectivities of 7% and 20% for p-polarized light around 520 - 530 nm were tested to evaluate their impact on system performance. Both gratings were purchased from Newport and feature 2400 grooves/mm. Wavelength adjustment is achieved by rotating the grating, as shown by the arrow in the sketch (Fig. 1). The laser diode is oriented such that its fast axis aligns with the diffraction plane, as indicated by the green arrow in Fig. 1. This configuration produces a wider beam across the diffraction grating for a given focal length, thereby increasing spectral resolution by illuminating more grooves. However, it also reduces first-order diffraction efficiency due to the p-polarization of the laser light, allowing higher laser output into the zeroth-order. To mitigate the system's sensitivity to temperature fluctuations, the temperature at the sub-mount is stabilized with an accuracy of 10 mK using a precision temperature controller. The spectrometer employed in this setup is an in-house developed and built high-dispersion grating spectrometer with long-focal-length lenses, specifically designed to meet our requirements by covering the spectral range of 505 to 541 nm while achieving a resolution of 0.025 nm. This resolution surpasses that of most conventional commercial

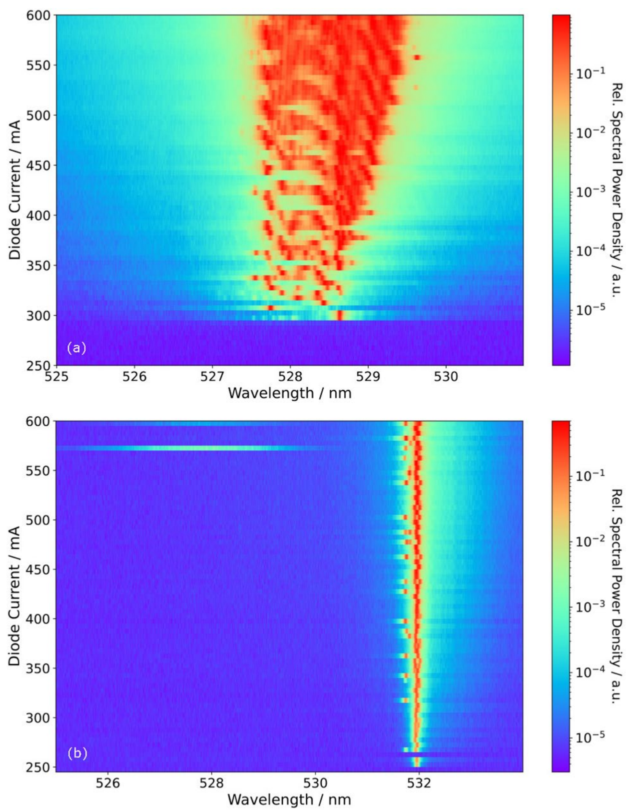

Fig. 2 Free-running emission spectra of diode A **a** and emission spectra of diode A in an external cavity setup with a 7% reflection grating tuned to 532 nm **b**. For both measurements, the injection current was incrementally increased and the emission spectrum recorded as a function of current. The resulting data are presented as a color map, with relative optical power indicated by the adjacent color bar

grating spectrometers, which typically sacrifice resolution in favor of a broader spectral range. The spectra presented in this work correspond to non-deconvolved data acquired directly from the spectrometer. Consequently, the measured linewidths are limited by the instrument's resolution. It is therefore reasonable to assume that the actual linewidth of the ECDL in single-mode operation can be narrower than the spectrometer's resolving capability.

To identify suitable candidates for Raman spectroscopy, eight laser diodes were systematically characterized within the external cavity setup. The selection comprised six broad-area multi-mode diodes and two transverse single-mode diodes. The diodes were labeled alphabetically. Table 1 summarizes the supplier, specified typical central wavelength, and diode type, designated as MM for broad-area multi-mode or SM for transverse single-mode, for each diode. Among the broad-area diodes, all but diode E provide maximum output power exceeding 1 W; diode E is rated at 300 mW. In contrast, the transverse single-mode diodes exhibit lower maximum output powers around 100 mW. For our intended application Raman spectroscopy we are targeting an optical power of the laser source of about 100 mW. Therefore, our investigations were focused on this power range, and we typically did not utilize the maximum possible output power of the broad-area diodes.

3 Measurements

All diodes underwent the same characterization process: Initially, the free-running emission spectra of each diode were recorded to determine their baseline emission profiles. Subsequently, the diodes were integrated into the external cavity setup and their tuning range was determined. Finally, wavelength-dependent measurements were conducted at multiple operating points, both with and without piezo-based correction of the external cavity length. Figure 2a shows the emission spectra of free running diode A at 20°C for an injection current range of 250 - 600 mA. The power bar in this and all subsequent color-map plots represents relative spectral power density in arbitrary units on a logarithmic scale, showing intensity variations within the plot (not absolute values). The laser diode emits a broad spectrum spanning 527.5 nm to 529.5 nm at 600 mA with a total optical output power of about 300 mW. With increasing current, a pronounced redshift of the spectrum is observed: the shorter-wavelength edge remains constant, while the longer-wavelength edge shifts progressively. This behavior aligns with findings from previous studies and is attributed to the redshift of the gain medium induced by elevated current and internal heating. [5, 6, 11]

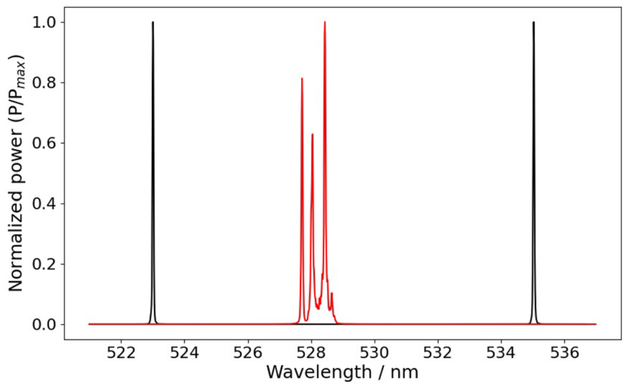

Fig. 3 Free-running emission (red) and stabilized emission at the spectral borders at 523 nm and 535 nm (black) of Diode A, all measured at an optical output power of 100 mW

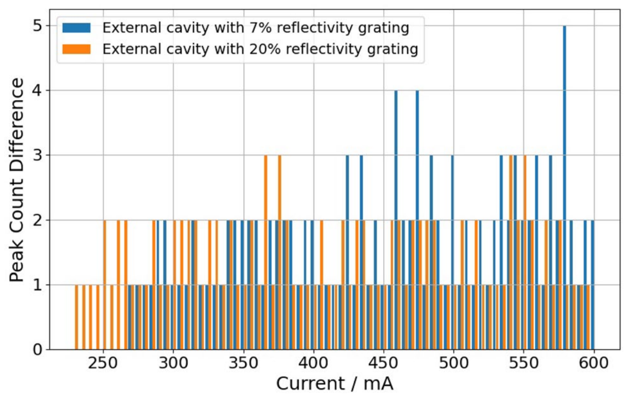

Fig. 4 Comparison of the number of detected longitudinal modes for the different gratings, measured at 532 nm using diode A

Subsequent measurements were conducted using the two diffraction gratings with diode A. Figure 3 shows the tunability of the laser diode at 100 mW output power within the external cavity setup using the grating with 20% reflectivity (black), with all power values normalized for comparison, compared to the free-running diode emission (red). The external cavity configuration significantly narrows the linewidth (FWHM = 0.04 nm) compared to the free-running diode (red curve in Fig. 3). Additionally, the tunable range extends beyond the diode's native emission spectrum. Based on the measured FWHM and the spectrometer resolution, we estimate an upper bound of 0.03 nm ($1\,\mathrm{cm}^{-1}$) for the true linewidth. As demonstrated by current instruments a spectral resolution around $6-8\,\mathrm{cm}^{-1}$ is sufficient for mineralogical analysis [16], making this linewidth fully adequate for planetary Raman spectroscopy applications. However, stable single-mode operation with a narrow linewidth was not achieved when the diode was fixed at a specific wavelength and the current incrementally increased, as shown in Fig. 2b. This measurement, taken at 20°C with the 7%-reflectivity grating and tuned to 532 nm, reveals the

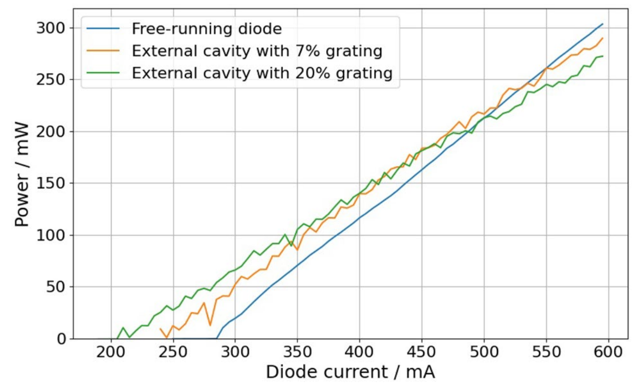

Fig. 5 Power over current plot of diode A in different setups. Blue: free-running diode, orange: diode in external cavity setup with 7% reflectivity grating, green: diode in external cavity setup with 20% reflectivity grating

presence of multiple longitudinal modes. Furthermore, at a diode current of approximately 570 mA, broad emission between 527 nm and 529 nm is observed, corresponding to the free-running diode emission (see Fig. 2a). Although this secondary emission is significantly weaker than the primary modes at 532 nm, it poses challenges for Raman spectroscopy. To assess the impact of grating reflectivity, the grating was replaced with one featuring 20% reflectivity. Figures 4 and 5 compare the performance of the two gratings at a fixed wavelength of 532 nm. Figure 4 plots the number of detected spectral peaks, each representing a longitudinal mode, against diode current. The 20%-reflectivity grating demonstrates a clear advantage by supporting fewer longitudinal modes across the current range.

Figure 5 presents the laser diode's output power as a function of current for three configurations: free-running (blue), external cavity with 7% grating (orange), and external cavity with 20% grating (green). The power fluctuations observed in the external-cavity operations are attributed to mode hopping. All configurations achieve maximum output powers between 250 mW and 300 mW in the set current range. It is important to note that the free-running diode can easily exceed 1 W output power at higher currents. However, the power was intentionally limited to this range, as the reduced output power is not only sufficient for Raman measurements but also extends the diode's lifetime and also provides a safety margin for power degradation due to radiation exposure in space missions. The free-running diode demonstrates the highest efficiency but also the highest threshold current, followed by the 7%-reflectivity grating and, finally, the 20%-reflectivity grating, which exhibits the lowest threshold current. Considering the requirements of Raman spectroscopy, output powers exceeding 100 mW are typically unnecessary, since 10 - 35 mW are sufficient for our application [16, 22]. Thus the 20% reflectivity grating emerges as the optimal choice for this setup. It achieves both the highest electrical to optical conversion efficiency and more stable single-mode operation in the lower power range, due to increased optical feedback. As demonstrated in Fig. 2b, stable single-mode operation of the diode could not be maintained across a broad current range. To address this, a piezoelectric actuator (Piezo) was mounted behind the grating, enabling precise adjustment of the cavity length on the order of a few micrometers, as indicated by the arrow in Fig. 1. This modification allowed for dynamic stabilization of the system in single-mode operation.

Figure 6 presents measurements for diode A at 20°C, with the Piezo stabilization tuned to 532 nm. It confirms that Piezo control enables single-mode operation across the entire current range, from the threshold current up to 600 mA. Within this range, the diode remained locked to a single longitudinal mode within approximately 50 mA wide injection current regions before experiencing a mode hop. To achieve stable single-mode operation, the Piezo voltage currently requires manual adjustment at each current step. While this process is time-consuming, it already significantly improves stability compared to measurements without Piezo stabilization, with the system typically remaining stable for tens of seconds to a few minutes. Future implementation of an automated control loop will further enhance both speed and long-term stability, eliminating temporal drift and ensuring permanent output consistency, a critical requirement for space applications. At elevated operating temperatures, even with Piezo tuning, single-mode operation cannot be sustained across the full current range. Specifically, at certain diode currents, multiple longitudinal modes emerge. However, at 40°C, the current range for stable single-mode operation remains broader than 200 mA, but decreases to just 50 mA at 60°C. Similar behavior was observed at other wavelengths, though with minor variations in the current ranges. These differences are too subtle to establish clear trends related to wavelength dependence. The only noticeable trend is that stability deteriorates at the edges of the tuning range, where only narrower current ranges remain tunable.

The same measurement protocol was applied to the remaining seven diodes, and their performance was subsequently compared. In free-running mode, all diodes exhibited broad spectral emission, with multiple longitudinal modes. The tuning ranges of the diodes are presented in Fig. 7. The green bars indicate the tuning range of each diode at the minimum current required for stable laser operation within the external cavity setup. This current is below the threshold current of the free-running diode, meaning the diode does not provide enough gain for its internal modes in this regime. Consequently, only modes of the external resonator are possible. Since each diode transitions from LED-like emission to lasing at a different current level,

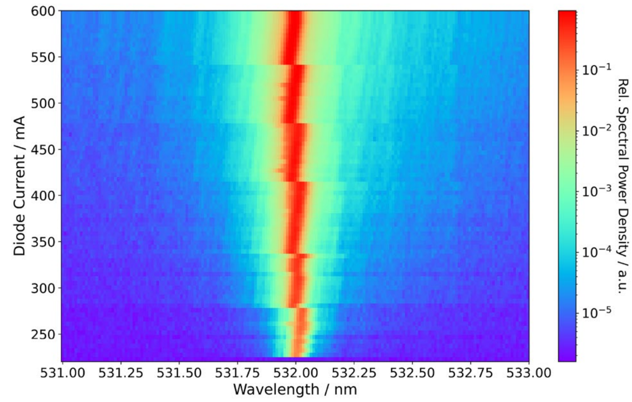

Fig. 6 Color map of longitudinal single-mode spectra recorded while increasing the diode current step-wise. The Piezo actuator was used to dynamically adjust the external cavity length, maintaining single-mode operation across as many current steps as possible

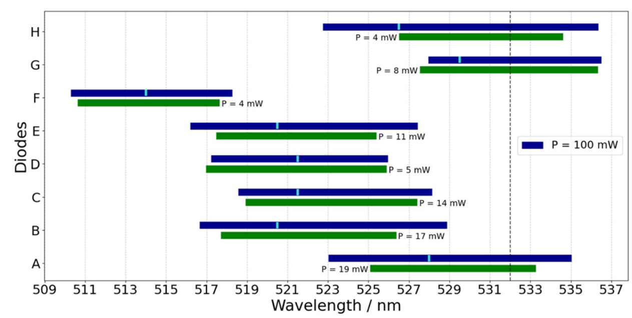

Fig. 7 Tuning ranges of the eight investigated diodes measured at the minimum stable optical power (lowest power at which the ECDL system operates stably and a tuning range can be observed, green bars) and at an optical power of 100 mW (darkblue bars). Diode D was evaluated at 80% of its maximum power (45 mW) due to its limited output

the individual current and corresponding output power are specified for each diode next to the green bars. The dark blue bars represent the tuning range at an output power of 100 mW and the turquoise lines mark the center of the free-running emission at 100 mW output power, allowing a direct comparison between the tunability and the center wavelength of the free-running emission.

All diodes, except diode D, achieved the 100 mW target power level. Diode D reached a maximum output power of 45 mW, so its tuning range was evaluated at 80% of its maximum power. Interestingly, diodes D and G were the only diodes whose tuning range did not increase with higher output power. The minimum tuning range observed at 100 mW was 8 nm (diode F). The broad-area diodes demonstrated larger tuning ranges of 10 to 12 nm, exceeding those of the transverse single-mode diodes. Among the diodes tested, only diodes A, G and H reached the desired wavelength of 532 nm, with diode H additionally exhibiting the largest tuning range of 14 nm. Notably, the tuning range of the broad-area diodes is asymmetric with respect to their central emission wavelength, allowing for greater tunability toward longer wavelengths than toward shorter ones.

In contrast, the transverse single-mode diodes show a symmetric tuning range centered around their nominal emission wavelength. Since the tuning range at low power current is smaller than at 100 mW power this limitation likely constrains the usable wavelength range in this configuration. The broad-area diodes B, C, E, and H exhibited consistent behavior with diode A, not only in their tuning ranges but also across other measurements. Meaning, using the Piezo actuator, it was possible to stabilize the longitudinal single-mode emission exceeding 100 mW output power. In contrast, the two transverse single-mode diodes (D and F) displayed distinct characteristics compared to the broad-area diodes, as exemplified by the measurements of diode D. Figure 8a shows measurements of diode D with the 20%-reflectivity grating, adjusted to 525 nm, near the upper limit of its tuning range, without Piezo stabilization. This diode achieved a maximum output power of 45 mW and operated within a lower current range (up to 150 mA). Interestingly, up to 120 mA, only one longitudinal mode was visible at any given time, though the system alternated between different modes depending on the current. Nevertheless, measurements with Piezo adjustment were conducted to avoid mode-hopping and to stabilize it within the same mode across as many current steps as possible. Figure 8b confirms that, similar to diode A, diode D could be locked to a single longitudinal mode for a current range of 50 mA. Diode F, the second transverse single-mode diode, is specified for a higher maximum output power of 130 mW. At moderate powers (up to 50 mW), it behaved similarly to diode D, exhibiting single-mode operation without Piezo correction. At higher powers, residual free-running emission became visible, but single-mode operation up to 100 mW was achieved with Piezo adjustment.

Last, Diode G is a broad-area diode with the highest specified emission wavelength of 532 nm. Unlike the other broad-area diodes tested, Diode G exhibited multiple longitudinal modes oscillating simultaneously already at threshold current (Fig. 9), rather than a single dominant mode (Fig. 2). While the beam could be collimated the same way as the other diodes, stabilization in the external cavity remained difficult. This manifested in both a reduced tuning range and a limited current range of 70 mA for stable longitudinal mode control via the Piezo actuator, a range fully sufficient for Raman measurements. Even at higher currents, spectral narrowing to 0.2 nm ($7\,\mathrm{cm}^{-1}$) was still achievable. Depending on the specific resolution requirements, this level of spectral resolution would still enable Raman measurements, thus providing a buffer against potential radiation-induced performance degradation. For comparison, both the Raman Laser Spectrometer (RLS) on board the ExoMars rover and

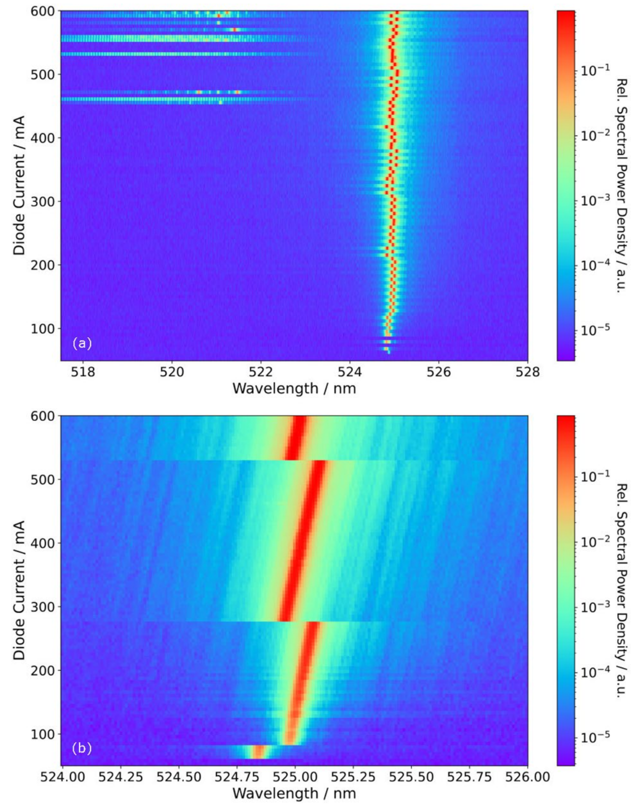

Fig. 8 Spectral emission of diode D in an external-cavity setup tuned to 525 nm. **a** Without Piezo adjustment of the cavity length, illustrating the natural tuning behavior under fixed cavity conditions. **b** With active Piezo adjustment of the cavity length, minimizing mode hopping and maintaining stable single-mode operation over extended current ranges. The wavelength range on the x-axis is chosen here narrower compared to **a** to highlight the stabilized emission

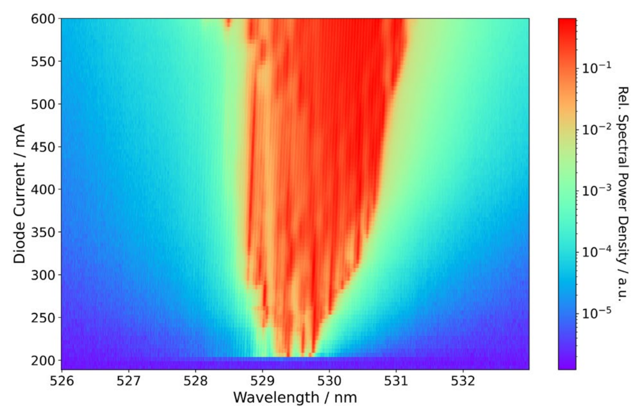

Fig. 9 Spectral emission of diode G in free-running operation at a constant temperature of 20°C, recorded while increasing the current step-wise. The measurement illustrates the emission behavior without external cavity stabilization

the laser of the RAX Raman Spectrometer for the MMX mission operate with a spectral resolution of $6-8\,\mathrm{cm}^{-1}$ [16, 19], demonstrating that this resolution is adequate for planetary and geological Raman applications. The initially possessed challenges achieving stable single-mode operation within the external-cavity setup could be resolved by replacing the initial lens (f = 4.6 mm, NA = 0.5) with one of longer focal length (f = 6.24 mm, NA = 0.42), resulting in an improved tuning range (Fig. 7) and stable behavior. Notably, the longer focal length increased the beam diameter, illuminating more grating lines and spectrally narrowing the feedback into the diode, an effect that may contribute to the observed stability. To further elucidate the influence of lens parameters on external-cavity performance, additional measurements and comparative studies are required. Such investigations could clarify why certain diodes perform better or worse in these setups, ultimately informing optimized designs for space-based Raman spectroscopy.

To validate the external cavity setup for its primary application, initial Raman measurements were conducted using diode A at 532 nm, the common wavelength for green laser-based Raman spectroscopy. The setup employed the 20%-reflectivity grating and Piezo stabilization. Laser stability and single-mode operation were monitored using our home-built high-resolution spectrometer, while Raman spectra were recorded with a conventional Avantes AvaSpec-Mini spectrometer (slit width = 10 µm, resolution = 0.3 nm, grating = 600 lines/mm). Measurements were performed with an integration time of 10 s, 10 accumulations and an excitation power of 20 mW. Figure 10 presents the results for various samples, confirming that Raman spectroscopy is feasible with this green ECDL setup. Although single-mode operation was unstable over the entire integration time and required manual Piezo readjustment, the characteristic Raman peaks of each sample were clearly identifiable. This demonstrates that the external-cavity setup is suitable for Raman measurements, even under challenging operational conditions.

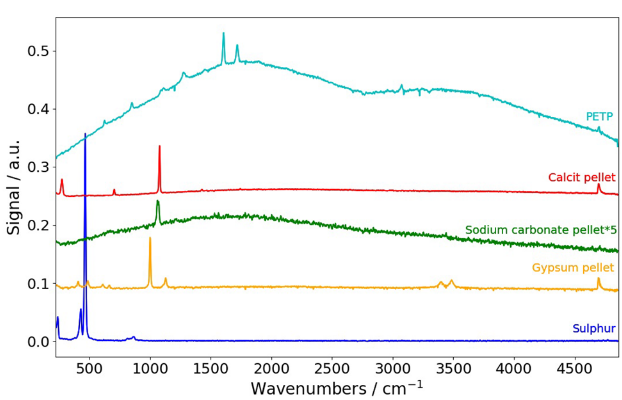

Fig. 10 Raman measurements of selected samples using diode A in an external-cavity setup. The signal intensity is presented in arbitrary units and normalized across all spectra for comparative analysis

4 Discussion

In this study, we characterized and evaluated green external-cavity diode lasers (ECDLs) in Littrow configuration for their suitability in Raman spectroscopy, with a particular focus on space-borne applications. The compact size, efficiency, and spectral tunability of these systems make them a compelling alternative to traditional solid-state lasers. In particular, green diodes operating at 532 nm are directly compatible with existing planetary instruments such as the RAX Raman spectrometer aboard MMX mission rover IDEFIX that will launch end of 2026. Additionally, by using green diodes tunable to 532 nm, we enable seamless compatibility with off-the-shelf optical filters, avoiding the need for custom components and reducing system complexity. The Littrow configuration was selected due to its simplicity and established reliability for initial testing and characterization of the diodes and ECDL system. Although this setup already meets space size constraints (a few centimeters dimension), automated cavity alignment and thermal management improvements are needed for long-term stability. Our results confirm its intended operation, establishing a strong basis for future work.

4.1 Wavelength coverage and tuning behavior

Our findings reveal distinct differences in the tuning behavior of the transverse multi-mode (MM) and transverse single-mode (SM) diodes. The tested MM diodes exhibited larger, asymmetric tuning ranges of 10 nm to 14 nm, with greater tunability toward longer wavelengths. This aligns with published data for green diode lasers, which typically report tuning ranges of 10 nm [5, 7]. Three MM diodes (A, G and H) reached the target wavelength of 532 nm, making them direct candidates for replacing frequency-doubled Nd:YAG lasers in Raman spectrometers. Notably, these diodes already achieve a narrower linewidth in single-mode operation, within the power range required for Raman spectroscopy, than the $6\,\mathrm{cm}^{-1}$ linewidth of the laser currently integrated into the RAX spectrometer [16, 19]. This suggests potential for improved spectral resolution in future space missions. The tested SM diodes, while not reaching 532 nm, demonstrated symmetric tuning behavior and enhanced mode stability, which may allow for simplified operation, potentially maintaining single-mode emission through temperature and current control alone, without Piezo stabilization. The measured tuning ranges at 100 mW output power are listed in Table 2 and shown in Fig. 7, whereas Fig. 11 provides a simplified schematic of the tuning behavior for illustrative purposes.

Table 2 Overview of diode characteristics. Diode D was evaluated at 45 mW (80% of its maximum power) due to its limited output

Name	Specified wavelength (Supplier)	Wavelength at 100mW	Tuning range at 100mW
A	530nm	528nm	523.0–535.0nm
B	525nm	520.5nm	516.7–528.9nm
C	520nm	521.5nm	518.6–528.1nm
D	520nm	521.5nm	517.2–526.0nm
E	520nm	520.5nm	516.2–527.4nm
F	520nm	514.0nm	510.3–518.3nm
G	532nm	529.5nm	527.9–536.5nm
H	530nm	526.5nm	522.7–536.4nm

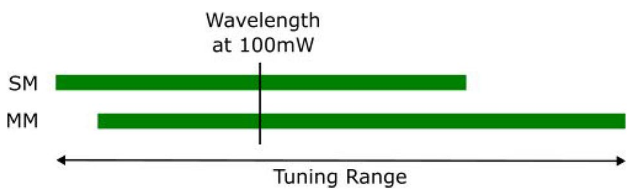

Fig. 11 Schematic comparison of tuning behavior between transverse multi-mode (MM) and single-mode (SM) diodes. MM diodes exhibit larger, asymmetric tuning ranges (10–14 nm), while SM diodes show symmetric tuning with enhanced mode stability

4.2 Operational stability and Raman performance

While single-mode operation currently requires manual Piezo adjustment, our system successfully identified characteristic Raman peaks of all tested samples, including minerals and PETP, confirming its suitability for Raman spectroscopy. In this first test setup, no optical isolation (e.g., a Faraday isolator) was used. Importantly, the observed instabilities in the laser system were not correlated with sample placement or removal. Stability issues persisted both with and without samples, suggesting that back-reflections from the samples were not the root cause. Nevertheless, a critical aspect for future investigations remains the potential destabilization caused by back-reflections from the sample into the laser cavity. Since the ECDL relies on grating feedback, such reflections could disrupt longitudinal single-mode operation. While our initial measurements did not conclusively determine the extent of this effect, further studies are needed to assess its impact. However, we assume that an optical isolator will be required, particularly when analyzing samples with higher reflectivity or complex optical properties.

4.3 Power and lifetime considerations

By limiting the output power of the broad-area diodes, we ensured sufficient performance for Raman measurements while extending diode lifetime and providing a buffer against radiation-induced degradation, which is a critical aspect for future space-borne applications. This conservative approach also offers a safety margin for potential power fluctuations during mission operations.

5 Conclusion

This study demonstrates the suitability of green external-cavity diode lasers (ECDLs) in Littrow configuration for Raman spectroscopy, particularly at 532 nm, offering compact size, efficiency, and possible compatibility with existing instruments like the RAX spectrometer. While transverse multi-mode diodes achieved asymmetric tuning ranges up to 14 nm and met the 532 nm target, single-mode diodes (SM) showed enhanced stability. Building on these results, the ECDL setup will undergo further refinements to enhance its robustness and suitability for space deployment.

Author contributions Data curation and analysis: J.L. Conceptualization, Investigation and Methodology: J.L. and E.D. Project administration: all authors Supervision: E.D., S.Sch. and H.-W. H. Writing - original draft: J.L. Writing – review and editing: all authors

Funding Open Access funding enabled and organized by Projekt DEAL.

Data availability Upon reasonable request, the corresponding author will provide access to the data underlying the results presented in this study.

Declarations

Conflict of interest The authors declare no conflict of interest.

References

1. S.M. Angel, M. Carrabba, T.F. Cooney, The utilization of diode lasers for Raman spectroscopy. Spectrochim. Acta Part A Mol. Biomol. Spectrosc. **51**(11), 1779–1799 (1995). https://doi.org/10.1016/0584-8539(95)01443-X
2. OSRAM Opto Semiconductors GmbH: Visible Laser Diodes. (2022). https://look.ams-osram.com/m/754d706b4e4fb0a/original/Flyer-Visible-Laser-EN.pdf
3" GrobidStyleApplied="Changed. Laser focus world: tunable semiconductor sources: scientific applications benefit from

external-cavity diode lasers (2010). https://www.laserfocusworld.com/test-measurement/research/article/16552023/tunable-semiconductor
4. W. Wang, A. Major, J. Paliwal, Grating-stabilized external cavity diode lasers for Raman spectroscopy–a review. Appl. Spectrosc. Rev. **47**(2), 116–143 (2012). https://doi.org/10.1080/05704928.2011.631649
5. M. Chi, O.B. Jensen, P.M. Petersen, Green high-power tunable external-cavity GaN diode laser at 515 nm. Opt. Lett. **41**(18), 4154 (2016). https://doi.org/10.1364/ol.41.004154
6. D. Ding, X. Lv, X. Chen et al., Tunable high-power blue external cavity semiconductor laser. Opt. Laser Technol. **94**, 1–5 (2017). https://doi.org/10.1016/j.optlastec.2017.03.015
7. Y.-H. Chen, W.-C. Lin, H.-Z. Chen et al., Single-frequency external cavity green diode laser. IEEE Photonics J. **9**(6), 1–7 (2017). https://doi.org/10.1109/jphot.2017.2776284
8. M. Chi, O.B. Jensen, A.K. Hansen, P.M. Petersen, Dynamics of a green high-power tunable external-cavity broad-area GaN diode laser. J. Opt. Soc. Am. B **35**(4), 667 (2018). https://doi.org/10.1364/josab.35.000667
9. Y. Zhu, B. Qiu, W. Li, Z. Liu, Mode-hop-free synchronous tuning range extension of an uncoated external cavity diode laser based on PZT hysteresis characteristic compensation. Appl. Phys. B **130**(11), 123 (2024). https://doi.org/10.1007/s00340-024-08342-6
10. N. Ruhnke, A. Müller, B. Eppich et al., 400 mW external cavity diode laser with narrowband emission at 445 nm. Opt. Lett. **39**(13), 3794 (2014). https://doi.org/10.1364/ol.39.003794
11. M. Chi, O.B. Jensen, P.M. Petersen, Tuning range and output power optimization of an external-cavity GaN diode laser at 455 nm. Appl. Opt. **55**(9), 2263 (2016). https://doi.org/10.1364/ao.55.002263
12. K. Sowoidnich, S. Pätzold, M. Ostermann et al., Qualitative and quantitative soil characterization on an agricultural field using a portable shifted excitation Raman difference spectroscopy instrument. Analyst **150**(13), 2934–2944 (2025). https://doi.org/10.1039/d5an00178a
13. S. Maurice, R.C. Wiens, P. Bernardi et al., The SuperCam instrument suite on the Mars 2020 rover: science objectives and mast-unit description. Space Sci. Rev. **217**(3), 47 (2021). https://doi.org/10.1007/s11214-021-00807-w
14. R.C. Wiens, S. Maurice, S.H. Robinson et al., The SuperCam instrument suite on the NASA Mars 2020 rover: body unit and combined system tests. Space Sci. Rev. **217**(1), 4 (2020). https://doi.org/10.1007/s11214-020-00777-5
15. R. Bhartia, L.W. Beegle, L. DeFlores et al., Perseverance's scanning habitable environments with Raman and Luminescence for organics and chemicals (SHERLOC) investigation. Space Sci. Rev. **217**(4), 58 (2021). https://doi.org/10.1007/s11214-021-00812-z
16. F. Rull, S. Maurice, I. Hutchinson et al., The Raman laser spectrometer for the ExoMars rover mission to Mars. Astrobiology **17**(6–7), 627–654 (2017). https://doi.org/10.1089/ast.2016.1567
17. Y. Cho, U. Böttger, F. Rull et al., In situ science on Phobos with the Raman spectrometer for MMX (RAX): preliminary design and feasibility of Raman measurements. Earth, Planets and Space **73**(1), 232 (2021). https://doi.org/10.1186/s40623-021-01496-z
18. S. Schröder, U. Böttger, M. Buder et al., RAX: The Raman Spectrometer on the MMX Rover for in-situ Surface Analysis on Phobos. In: LPSC 2023 (2023)
19. S. Schröder, U. Böttger, Y. Cho et al., The Raman spectrometer RAX on the MMX IDEFIX rover for in-situ mineralogical analysis on phobos. In: Europlanet Science Congress 2024, Berlin, Germany (2024). https://doi.org/10.5194/epsc2024-988 . EPSC2024-988
20. S. Ulamec, P. Michel, N. Murdoch et al., Science operations of IDEFIX, the MMX Phobos rover. Prog Earth Planet Sci **12**(1), 97 (2025). https://doi.org/10.1186/s40645-025-00771-x
21. P. Ribes-Pleguezuelo, D. Guilhot, M. Gilaberte Basset et al., Insights of the qualified ExoMars laser and mechanical considerations of its assembly process. Instruments **3**(2), 25 (2019). https://doi.org/10.3390/instruments3020025
22. E. Beckert, P.R. Perez, G. Rosario-Rodriguez, M. Benito-Parejo, Soldering of optics for the 532 nm, 100 mW raman laser for JAXA's mission to Phobos, and for ExoMars. In: Components and Packaging for Laser Systems X (2024). https://doi.org/10.1117/12.3003779 . International Society for Optics and Photonics
23. E.A. Cloutis, C. Caudill, E.A. Lalla, LunaR: overview of a versatile Raman spectrometer for lunar exploration. Front. Astron. Space Sci. **9**, 1016359 (2022). https://doi.org/10.3389/fspas.2022.1016359